GEOPHYSICS, VOL. 66, NO. 4 (JULY-AUGUST 2001); P. 1141–1148, 7 FIGS., 1 TABLE.

A semianalytical solution for the propagation of electromagnetic waves in 3-D lossy orthotropic media

José M. Carcione and Fabio Cavallini*

ABSTRACT

We derive an analytical solution for electromagnetic waves propagating in a 3-D lossy orthotropic medium for which the electric permittivity tensor is proportional to the magnetic permeability tensor. The solution is obtained through a change of coordinates that transforms the spatial differential operator into a pure Laplace operator and the differential equations for the electric and magnetic field components into pure Helmholtz equations. A plane-wave analysis gives the expression of the slowness and attenuation surfaces as a function of frequency and propagation direction. The transverse electric and transverse magnetic surfaces degenerate to one repeated sheet so that, in any direction, the two differently polarized plane waves have the same slowness. A computer experiment with realistic geophysical parameters has shown that the anisotropic propagation and dissipation properties emerging from plane-wave analysis agree with the different time histories of the magnetic field computed at a number of representative receiver locations.

INTRODUCTION

The high and growing interest in the use of ground-penetrating radar (GPR) for imaging underground structures has been a strong motivation for research on high-frequency electromagnetic (EM) wave propagation in rocks. It is well known from laboratory and field measurements that in practical applications low values of the quality factor Q arise. Moreover, electric and magnetic anisotropy are also to be taken into account. Therefore, computer codes for GPR wave simulation are getting more and more complex. The problem of their validation is more crucial than ever, and this in turn has produced a revival of interest in the search for analytical solutions to be used as benchmarks for numerical simulations (at least in the case of homogeneous media and simplified geometries).

Modeling EM waves in a realistic medium requires the correct description of the anisotropic properties and of the different dissipation mechanisms. For instance, anisotropy may be important at different scales (Negi and Saraf, 1989): intrinsic anisotropy, composite media made of fine layers compared to the pulse wavelength, and fluid-filled cracks and fractures give rise to electric and magnetic anisotropy. Similarly, the presence of mineralized water in the fractures causes anisotropy in the electric conductivity. On the other hand, dissipation may be caused by different relaxation mechanisms as, for instance, water relaxation and ferromagnetic domain relaxation. The presence of out-of-phase currents is a peculiar feature of these modified dielectric properties.

In general, for media of arbitrary geometrical features, the EM field can only be calculated numerically (e.g., Carcione, 1996). But, as stated before, analytical solutions are essential to verify the accuracy of modeling algorithms, especially for what concerns numerical dispersion in space or time and plain coding errors. Yet other possible errors, related to source implementation and boundary and interface conditions, may not be detected this way. In the following sections, we obtain a closed-form analytical solution for time-harmonic wave propagation in a particular class of orthotropic media, for which the permittivity tensor is proportional to the magnetic permeability tensor, both complex and frequency dependent. Because of the assumed relationship between permittivity and permeability, one may argue that our solution is not to be viewed as a fully realistic model of a geologic material. We partly agree, but we stress that the numeric values of the pertinent parameters have been chosen within geophysical ranges (see Table 1); moreover, constitutive laws satisfying our assumption play a crucial role in the realistic modeling of geologic materials when using the perfectly matched layer (PML) technique (Teixeira and Chew, 1997, and 1998).

Finally, a plane-wave analysis (see Appendix) will show that this class of media has coincident transverse electric (TE) and transverse magnetic (TM) slowness curves.

Manuscript received by the Editor September 30, 1997; revised manuscript received November 2, 2000.
*Istituto Nazionale di Oceanografia e di Geofisica Sperimentale (OGS) Borgo Grotta Gigante 42/C, I-34010 Sgonico, Trieste, Italy. E-mail: jcarcione@ogs.trieste.it; fcavallini@ogs.trieste.it.

MAXWELL'S AND WAVE EQUATIONS

Maxwell's equations for a nondispersive inhomogeneous anisotropic medium yield a single vector wave equation for the magnetic field (Chew, 1990, p. 17):

$$\mu \cdot \frac{\partial^2 H}{\partial t^2} = \nabla \times \epsilon^{-1} \cdot (J - \nabla \times H), \tag{1}$$

where H is the magnetic field, J is the current density, μ is the magnetic permeability tensor, ϵ is the electric permittivity tensor, and t is time.

Dielectric relaxation processes give rise to out-of-phase conduction currents (Carcione, 1996), and magnetic losses occur in media with ferromagnetic domain relaxation and superparamagnetic relaxation (Olhoeft and Capron, 1994). To deal with these effects, the permeability and permittivity tensors must be taken as time dependent, and the constitutive relation between the electric induction D and the electric field E becomes $D = \epsilon * E$, where ϵ now denotes the time derivative of the electric permittivity and the asterisk denotes convolution in time, analogously for the constitutive relation between the magnetic induction and the magnetic field. Thus, equation (1) becomes

$$\mu * \frac{\partial^2 H}{\partial t^2} = \nabla \times \epsilon^{\leftarrow} * (J - \nabla \times H), \tag{2}$$

where the superscript $\leftarrow$ denotes the inverse with respect to convolution. Equivalently, the frequency-domain formulation of equation (2) is

$$-\omega^2 \boldsymbol{\mu} \cdot \mathbf{H} = \nabla \times \boldsymbol{\epsilon}^{-1} \cdot (\mathbf{J} - \nabla \times \mathbf{H}), \tag{3}$$

where ω is the angular frequency, while $\mathbf{H}$, $\mathbf{J}$, $\boldsymbol{\mu}$, and $\boldsymbol{\epsilon}$ are the Fourier-transformed counterparts of H, J, μ, and ϵ, respectively.

We assume now that the medium is homogeneous. However, even in this situation the tensors ϵ^{-1} and $\boldsymbol{\mu}$ do not commute with the $\nabla\times$ operator. We further assume that the medium is orthotropic and that its principal system coincides with the Cartesian system where the problem is solved. In orthotropic media, the eigenvectors of the material tensors coincide, allowing these tensors to have the form

$$\boldsymbol{\epsilon} = \begin{pmatrix} \epsilon_1 & 0 & 0 \\ 0 & \epsilon_2 & 0 \\ 0 & 0 & \epsilon_3 \end{pmatrix}, \qquad \boldsymbol{\mu} = \begin{pmatrix} \mu_1 & 0 & 0 \\ 0 & \mu_2 & 0 \\ 0 & 0 & \mu_3 \end{pmatrix}. \tag{4}$$

In Cartesian coordinates, the magnetic field is $\mathbf{H} = (H_x, H_y, H_z)$, and the vector term $\nabla \times \boldsymbol{\epsilon}^{-1} \cdot \nabla \times \mathbf{H}$ consists of three scalar terms:

$$\epsilon_3^{-1}\left(\partial_x \partial_y H_y - \partial_y^2 H_x\right) - \epsilon_2^{-1}\left(\partial_z^2 H_x - \partial_x \partial_z H_z\right), \tag{5}$$

$$\epsilon_1^{-1}\left(\partial_y \partial_z H_z - \partial_z^2 H_y\right) - \epsilon_3^{-1}\left(\partial_x^2 H_y - \partial_x \partial_y H_x\right), \tag{6}$$

Table 1. Material properties.

$\epsilon_1^\infty(\epsilon_0)$	$\epsilon_2^\infty(\epsilon_0)$	$\epsilon_3^\infty(\epsilon_0)$	σ_1^0 (S/m)	σ_2^0 (S/m)	σ_3^0 (S/m)
1	1.5	2	0.025	0.05	0.025
Q_1^ϵ	Q_2^ϵ	Q_3^ϵ	χ_1	χ_2	χ_3
20	15	10	$0.2\epsilon_0/\sigma_1^0$	$0.2\epsilon_0/\sigma_2^0$	$0.2\epsilon_0/\sigma_3^0$
$\epsilon_0 = 8.85\ 10^{-12}$ F m^{-1}			$\mu_0 = 4\pi\ 10^{-7}$ H m^{-1}		

$$\epsilon_2^{-1}\left(\partial_x \partial_z H_x - \partial_x^2 H_z\right) - \epsilon_1^{-1}\left(\partial_y^2 H_z - \partial_y \partial_z H_y\right). \tag{7}$$

In the absence of magnetic current densities, we have $\nabla \cdot \mathbf{B} = 0$ (Chew, 1990), where $\mathbf{B} = \boldsymbol{\mu} \cdot \mathbf{H}$ is the magnetic flux vector. Then

$$\mu_1 \partial_x H_x + \mu_2 \partial_y H_y + \mu_3 \partial_z H_z = 0. \tag{8}$$

Using equations (5)–(8) and multiplying the three components of equation (3) by $-\epsilon_2\epsilon_3$, $-\epsilon_1\epsilon_3$, and $-\epsilon_1\epsilon_2$, respectively, yields

$$\frac{\mu_1}{\mu_2}\epsilon_2 \partial_x^2 H_x + \epsilon_2 \partial_y^2 H_x + \epsilon_3 \partial_z^2 H_x - \left(\epsilon_3 - \frac{\mu_3}{\mu_2}\epsilon_2\right)\partial_x \partial_z H_z + \omega^2 \mu_1 \epsilon_2 \epsilon_3 H_x = \epsilon_3 \partial_z J_y - \epsilon_2 \partial_y J_z, \tag{9}$$

$$\epsilon_1 \partial_x^2 H_y + \frac{\mu_2}{\mu_1}\epsilon_1 \partial_y^2 H_y + \epsilon_3 \partial_z^2 H_y - \left(\epsilon_3 - \frac{\mu_3}{\mu_1}\epsilon_1\right)\partial_y \partial_z H_z + \omega^2 \mu_2 \epsilon_1 \epsilon_3 H_y = \epsilon_1 \partial_x J_z - \epsilon_3 \partial_z J_x, \tag{10}$$

$$\epsilon_1 \partial_x^2 H_z + \epsilon_2 \partial_y^2 H_z + \frac{\mu_3}{\mu_1}\epsilon_1 \partial_z^2 H_z - \left(\epsilon_2 - \frac{\mu_2}{\mu_1}\epsilon_1\right)\partial_y \partial_z H_y + \omega^2 \mu_3 \epsilon_1 \epsilon_2 H_z = \epsilon_2 \partial_y J_x - \epsilon_1 \partial_x J_y. \tag{11}$$

As we shall see in the next section, the system of equations (9)–(11) can be solved in closed form by assuming the general permittivity tensor is proportional to the magnetic permeability tensor:

$$\boldsymbol{\epsilon} \propto \boldsymbol{\mu}. \tag{12}$$

This particular class of orthotropic media satisfies

$$\mu_1 \epsilon_2 = \mu_2 \epsilon_1, \qquad \mu_1 \epsilon_3 = \mu_3 \epsilon_1, \qquad \mu_2 \epsilon_3 = \mu_3 \epsilon_2. \tag{13}$$

This assumption is similar to one independently proposed (Lindell and Olyslager, 1997). Using these relations, the system of equations (9)–(11) can be written as a single vector equation:

$$\Delta_\epsilon \mathbf{H} + \omega^2 \eta \mathbf{H} = -\nabla_\epsilon \times \mathbf{J}, \tag{14}$$

where $\eta = \mu_1 \epsilon_2 \epsilon_3$ and

$$\Delta_\epsilon = \epsilon_1 \partial_x^2 + \epsilon_2 \partial_y^2 + \epsilon_3 \partial_z^2, \qquad \nabla_\epsilon = (\epsilon_1 \partial_x, \epsilon_2 \partial_y, \epsilon_3 \partial_z). \tag{15}$$

The equations for the electric field components can be obtained from equation (14) using duality (Chew, 1990, p. 9):

$$\Delta_\mu \mathbf{E} + \omega^2 \chi \mathbf{E} = \nabla_\mu \times \mathbf{M}, \tag{16}$$

where $\chi = \epsilon_1 \mu_2 \mu_3$ and

$$\Delta_\mu = \mu_1 \partial_x^2 + \mu_2 \partial_y^2 + \mu_3 \partial_z^2, \quad \nabla_\mu = (\mu_1 \partial_x,\ \mu_2 \partial_y,\ \mu_3 \partial_z). \tag{17}$$

Note that relations (13) are not modified by duality.

THE SOLUTION

The aim of this section is to solve the inhomogeneous Helmholtz-like equations (14) and (16) in the sense of distributions. To this purpose, we first compute the Green's function of the associated scalar equation and then convolve it with the source term (Carcione and Cavallini, 1993).

Change of coordinates.—The following change of coordinates,

$$x \to \alpha\sqrt{\epsilon_1}, \qquad y \to \beta\sqrt{\epsilon_2}, \qquad z \to \gamma\sqrt{\epsilon_3}, \tag{18}$$

transforms Δ_ϵ into a pure Laplacian differential operator. Rather surprisingly, a similar change of coordinates is also used in another context where permittivity and permeability are proportional, namely, in the synthesis of perfectly matched layer absorbing boundary conditions for EM waves (Teixeira and Chew, 1997, 1998). Using equation (18), the first component of equation (14) becomes

$$\Delta H_\alpha + \omega^2 \eta H_\alpha = \sqrt{\epsilon_3}\partial_\gamma J_\beta - \sqrt{\epsilon_2}\partial_\beta J_\gamma, \tag{19}$$

where $\Delta = \partial_\alpha^2 + \partial_\beta^2 + \partial_\gamma^2$ is the Laplace operator in the new coordinates and analogously for the other components.

Solution in the new coordinates.—Consider the equation for the Green's function of equation (19),

$$\Delta H_\alpha + \omega^2 \eta H_\alpha = -\delta(\rho), \tag{20}$$

whose solution is (Chew, 1990, p. 26)

$$g(\rho) = \frac{1}{4\pi\rho}\exp(\mathrm{i}\omega\rho\sqrt{\eta}), \tag{21}$$

where

$$\rho = \sqrt{\alpha^2 + \beta^2 + \gamma^2}. \tag{22}$$

The spatial derivatives of the electric currents in equation (19) imply the differentiation of the Green's function. Assume, for instance, that the electric currents J_β and J_γ are delta functions: $J_\beta = \bar{J}_\beta\delta[\rho]$ and $J_\gamma = \bar{J}_\gamma\delta[\rho]$. Since the solution of equation (19) is the convolution of the Green's function with the source term, it can be obtained as the β spatial derivative of the Green's function. Then, for electric currents that are nonzero at a single point (i.e., are Dirac's delta functions of space), the solution is

$$H_\alpha = -(\sqrt{\epsilon_3}\bar{J}_\beta\partial_\gamma g - \sqrt{\epsilon_2}\bar{J}_\gamma\partial_\beta g). \tag{23}$$

We have

$$\partial_\beta g = \frac{\beta}{\rho}\partial_\rho g, \qquad \partial_\gamma g = \frac{\gamma}{\rho}\partial_\rho g, \tag{24}$$

where

$$\partial_\rho g = -\left(\frac{1}{\rho} - \mathrm{i}\omega\sqrt{\eta}\right)g. \tag{25}$$

Solution in the old coordinates.—In terms of the original Cartesian coordinates, the solution is

$$H_x = \frac{1}{4\pi\rho^2}(z\bar{J}_y - y\bar{J}_z)\left(\frac{1}{\rho} - \mathrm{i}\omega\sqrt{\eta}\right)\exp(\mathrm{i}\omega\rho\sqrt{\eta}), \tag{26}$$

where

$$\rho = \left(\frac{x^2}{\epsilon_1} + \frac{y^2}{\epsilon_2} + \frac{z^2}{\epsilon_3}\right)^{1/2}. \tag{27}$$

Similarly, the other components are given by

$$H_y = \frac{1}{4\pi\rho^2}(x\bar{J}_z - z\bar{J}_x)\left(\frac{1}{\rho} - \mathrm{i}\omega\sqrt{\eta}\right)\exp(\mathrm{i}\omega\rho\sqrt{\eta}) \tag{28}$$

and

$$H_z = \frac{1}{4\pi\rho^2}(y\bar{J}_x - x\bar{J}_y)\left(\frac{1}{\rho} - \mathrm{i}\omega\sqrt{\eta}\right)\exp(\mathrm{i}\omega\rho\sqrt{\eta}). \tag{29}$$

The three components of the magnetic field are not functionally independent, since they must satisfy equation (8). (This functional dependence has also been verified by computing the Jacobian determinant of H_x, H_y, and H_z with a symbolic computer algebra code by the authors.)

Time-domain solution.—When solving the problem with a limited-band wavelet source $f(t)$, the frequency-domain solution is multiplied by the Fourier transform $F(\omega)$. To ensure a real time-domain solution, we consider an Hermitian frequency-domain solution. Finally, the time-domain solution is obtained by an inverse transform.

EXAMPLE AND DISCUSSION

In this section we solve wave equation (2) for a homogeneous medium that satisfies the condition

$$\mu = 2\frac{\mu_0}{\epsilon_0}\epsilon, \tag{30}$$

where the subscript 0 denotes vacuum (see Table 1).The following two subsections contain details on the permittivity tensor ϵ and the source vector J.

The permittivity tensor

The (effective) permittivity tensor may be expressed in the frequency domain as

$$\boldsymbol{\epsilon} = \boldsymbol{\epsilon}_R + \frac{\mathrm{i}}{\omega}\boldsymbol{\sigma}, \tag{31}$$

where $\boldsymbol{\epsilon}_R = \mathrm{diag}(\epsilon_{R1}, \epsilon_{R2}, \epsilon_{R3})$ and $\boldsymbol{\sigma} = \mathrm{diag}(\sigma_1, \sigma_2, \sigma_3)$ are the complex permittivity and conductivity tensors, explicitly describing dielectric relaxation processes and conductivity effects, respectively. We assume that the scalar permittivities in equation (31) are given by the Debye relaxation model,

$$\epsilon_{Ri} = \epsilon_i^\infty - \frac{\epsilon_i^\infty - \epsilon_i^0}{1 - \mathrm{i}\tau_i\omega} \qquad (i = 1, 2, 3), \tag{32}$$

where ϵ_i^0 and ϵ_i^∞ (with $\epsilon_i^\infty > \epsilon_i^0$) are the static and optical permittivities, respectively, and τ_i is a relaxation time. Likewise, the conductivity components can be written as

$$\sigma_i = \sigma_i^0(1 - \mathrm{i}\chi_i\omega), \tag{33}$$

where σ_i^0 is the dc conductivity and χ_i is a relaxation time quantifying the out-of-phase electric currents.

By straightforward computations analogous to the case of seismic waves (Casula and Carcione, 1992), the Debye complex modulus (32) can be written in terms of the minimum quality factor Q_i given at the frequency f_i. Then,

$$\epsilon_i^\infty = \epsilon_i^0\left(1 - \frac{2}{1 + \sqrt{1 + Q_i^2}}\right) \tag{34}$$

and

$$\tau_i = \frac{1}{2\pi f_i}\left(\frac{1}{Q_i} + \sqrt{1+\frac{1}{Q_i^2}}\right). \tag{35}$$

Table 1 lists the numerical values of the constitutive parameters affecting the permittivity tensor. Let us assume that the Debye mechanisms peak at $f_i = 250$ MHz for $i = 1, 2, 3$. Figure 1 shows sections of the slowness and attenuation surfaces across the principal planes for a frequency of 200 MHz. As anticipated in the Introduction and shown in the Appendix, the TM and TE curves obtained from a plane-wave analysis coincide for this type of orthotropic medium. The energy velocity is shown in Figure 2. This is calculated as the real part of the Umov-Poynting vector divided by the total energy density (e.g., Carcione, 1996) and is better suited than group velocity to describe wave propagation in dissipative media, as shown in Carcione (1994) and Carcione et al. (1996).

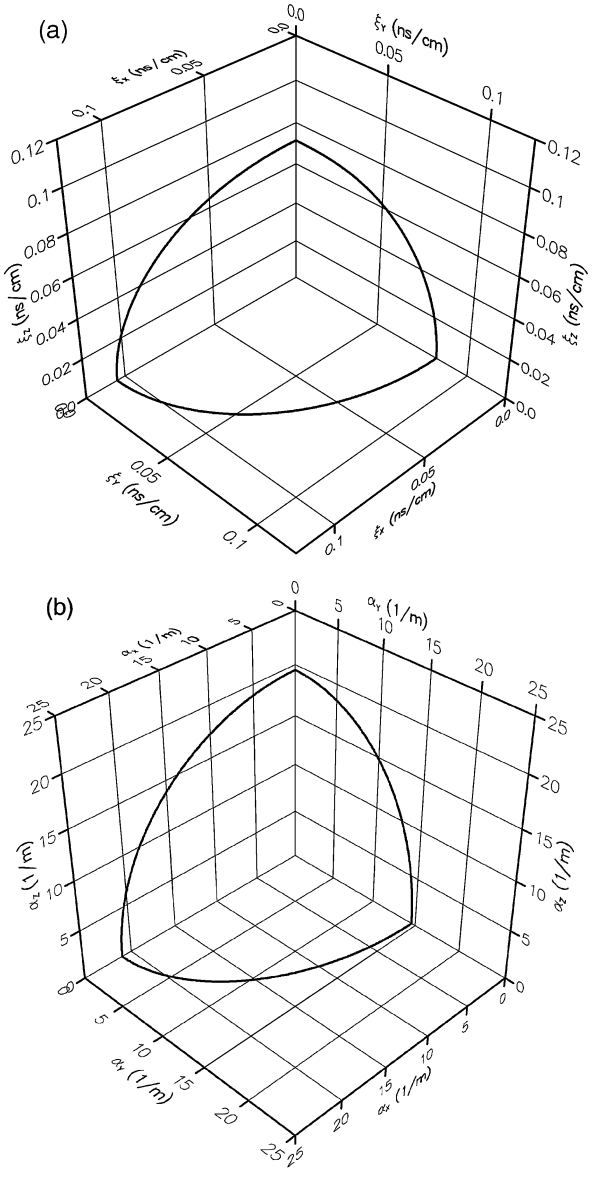

FIG. 1. (a) Slowness and (b) attenuation curves at the coordinate planes for a frequency of 250 MHz. The material properties are given in Table 1. Only one octant is shown from symmetry considerations.

The source

For computing the transient solution, we assume a source vector

$$J = h(t)\,(\bar{J}_x, \bar{J}_y, \bar{J}_z), \tag{36}$$

with $\bar{J}_x = \bar{J}_y = 0$, $\bar{J}_z = 1$ A/m^2, and

$$h(t) = \exp\left[-\frac{1}{2} f_c^2 (t-t_0)^2\right]\cos[\pi f_c (t-t_0)], \tag{37}$$

where f_c is the cutoff frequency and $t_0 = 3/f_c$. In the following computations the cutoff frequency of the source wavelet in equation (37) is $f_c = 250$ MHz. The response of the medium is obtained by multiplying the Green's functions (26), (28), and (29) by the time Fourier transform of the wavelet

$$\hat{h}(\omega) = \frac{\sqrt{2\pi}}{f_c}\exp\left[-\frac{1}{2}\left(\pi^2 + \frac{\omega^2}{f_c^2}\right)\right]\cos\mathrm{h}\left(\pi\frac{\omega}{f_c}\right)\exp(\mathrm{i}\,t_0\,\omega) \tag{38}$$

and then performing an inverse Fourier transform back to the time domain. We point out that, for dissipative media, the frequency-domain Green's function has a singularity at zero frequency which, a priori, seems troublesome. In our work we have overcome this problem by choosing a source whose Fourier transform has (for all practical purposes) a compact support not containing zero. In other words, here the vanishing of the source at low frequencies kills the singularity of the Green's function. But in general, this question requires careful treatment.

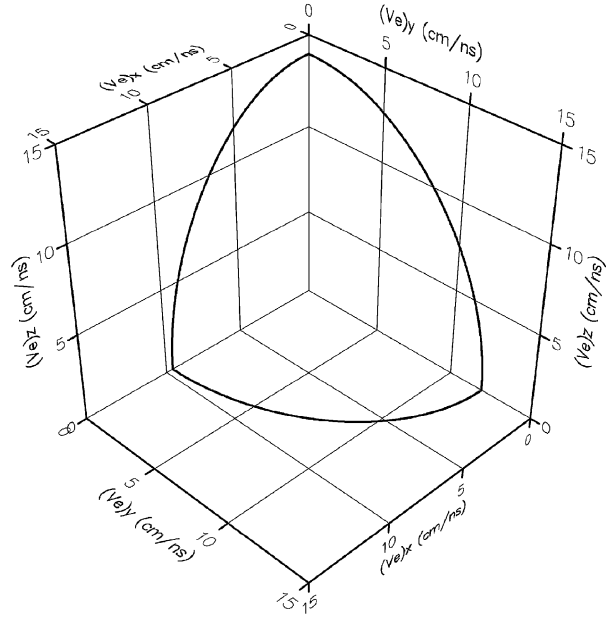

FIG. 2. Energy velocity curves at the coordinate planes for a frequency of 250 MHz. The material properties are given in Table 1. Only one octant is shown from symmetry considerations.

Results

Figure 3 shows the locations of receivers in a perspective view. Figure 4 represents the H_x solution at seven equidistant receiver points on a circle located in the first quadrant of the (x, y)-plane. Receiver 1 is located on the x-axis. A similar plot, corresponding to a circle contained in the plane $x = y$ and in the first octant of the 3-D space, is shown in Figure 5. Receiver 8 in Figure 5 coincides with receiver 4 in Figure 4.

As can be appreciated from Figures 4 and 5, the arrival times of the pulses agree with the anisotropic features of the energy velocity curve displayed in Figure 2. For example, Figure 2 shows that the energy velocity is higher along the y-axis than along the x-axis; indeed, receiver 7, located on the y-axis, sees the signal earlier than receiver 2, located near the x-axis. Moreover, each of Figures 2, 4, and 5 yields a propagation velocity of the order of 10 cm/ns, which is approximately one-third the speed of light in a vacuum.

The analysis of attenuation properties is not so straightforward because the decay of the signal is affected by the radiation pattern of the source and by the intrinsic dissipation properties of the medium. However, drawing figures similar to Figures 4 and 5 in the lossless case (not shown here for brevity) let us single out the effects of the radiation pattern. For example, from Figures 1 and 3 we see that attenuation is higher at receiver 2 than at receiver 7, and indeed the ratio between the peak values of the signal in the lossless and lossy cases is higher for receiver 2. As a consequence, we have found that the anisotropic dissipation properties illustrated by Figure 1 are in qualitative agreement with the attenuation of the signal shown in Figures 4 and 5. Figures 6 and 7 show polar plots of the signal amplitudes in the lossless and lossy cases. From these plots one can quantitatively appreciate the dissipation effects attributable to the complex permittivity tensor.

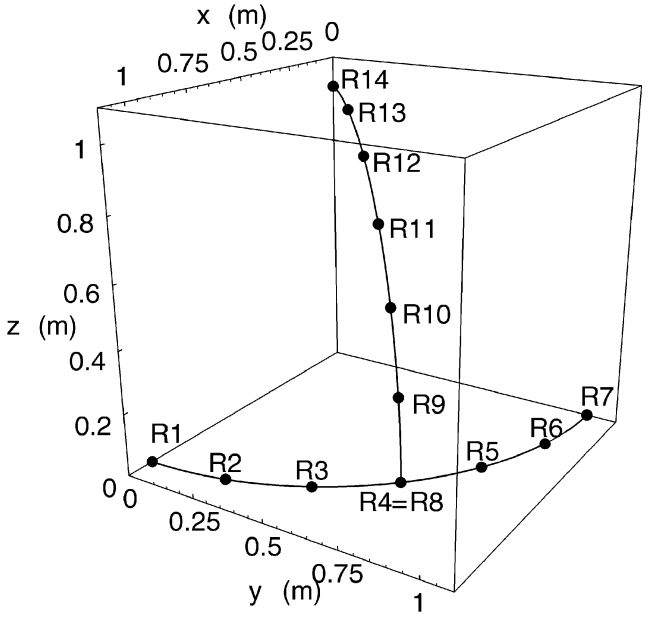

FIG. 3. Perspective view of the receiver positions where the synthetic signal, generated by a source located at the origin, has been detected. The corresponding recorded wavelets are shown in Figures 4 and 5.

CONCLUSIONS

We have considered a class of orthotropic media with a time-dependent source acting at a single point, and we have derived a semianalytical solution for the EM field through the following main steps:

1) Maxwell's equations for time-harmonic field components are decoupled by assuming proportionality between electric permittivity and magnetic permeability tensors;
2) a rescaling of the independent spatial variables transforms each of the resulting equations into a familiar Helmholtz equation whose known analytical solution gives the Green's function of our problem in the frequency domain;
3) the product between the frequency-domain Green's function and the Fourier transform of the source wavelet yields the frequency-domain solution; and
4) the time-domain solution is obtained as the inverse Fourier transform of the frequency-domain solution.

A computer experiment with realistic geophysical values for material properties has produced signal outputs whose anisotropic propagation and damping properties are qualitatively in agreement with the patterns of slowness, attenuation, and energy velocity arising from plane-wave analysis.

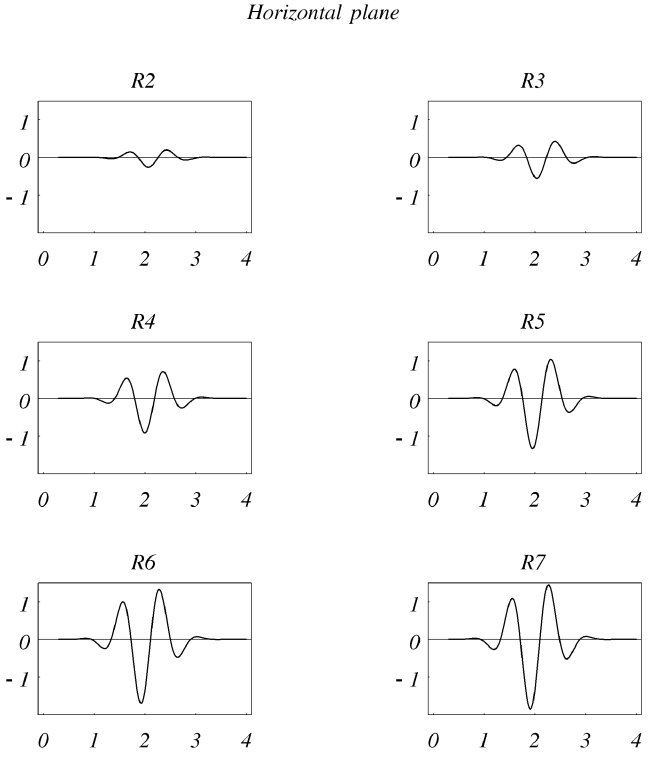

FIG. 4. Waveforms of the magnetic field component H_x computed at six equidistant receiver points on a circle (of radius $R = 1$ m) located in the first quadrant of the (x, y)-plane (see Figure 3). The response at the first receiver, located on the x-axis, is not shown because it is zero. In all plots, the abscissa represents time t expressed in seconds $\times 10^{-8}$. The ordinate represents the magnetic field component H_x expressed in (A/m) $\times 10^{-17}$.

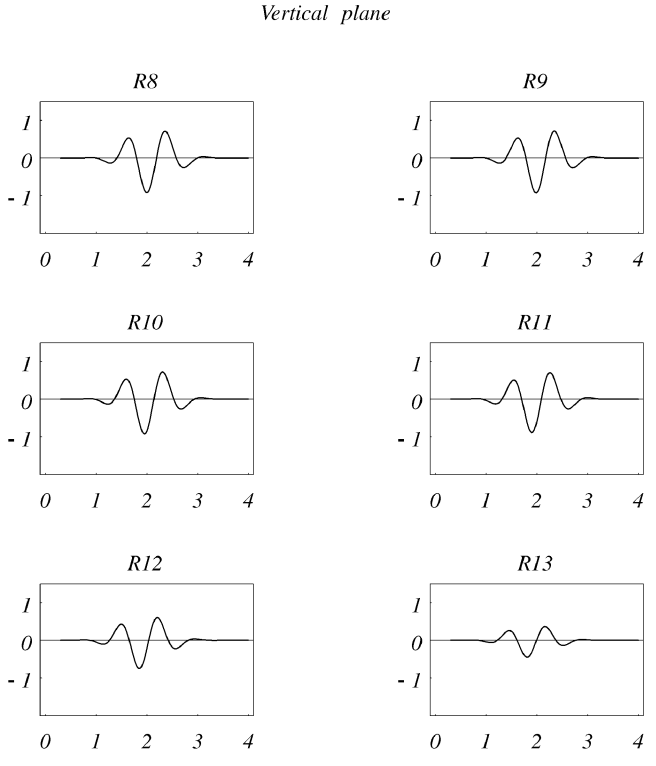

FIG. 5. Same as Figure 4, but here the receivers are located on a circle contained in the plane $x = y$ and in the first octant of the 3-D space (see Figure 3). The response at receiver 14, located on the z-axis, is not shown because it is zero.

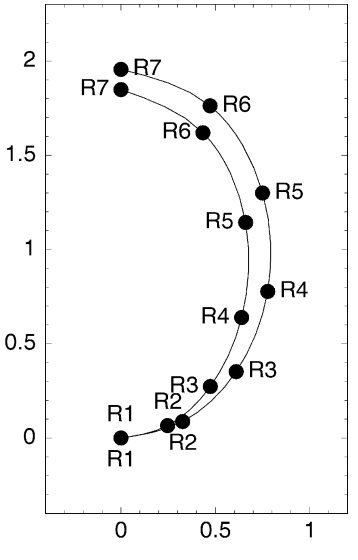

FIG. 6. Polar plot of the signal amplitude for the magnetic field component H_x at receivers 1–7 (see Figure 3). The inner and outer curves correspond to the lossy and lossless cases, respectively. The interpolation curves are cubic splines. The physical units on the axes are expressed in $(\mathrm{A/m}) \times 10^{-17}$.

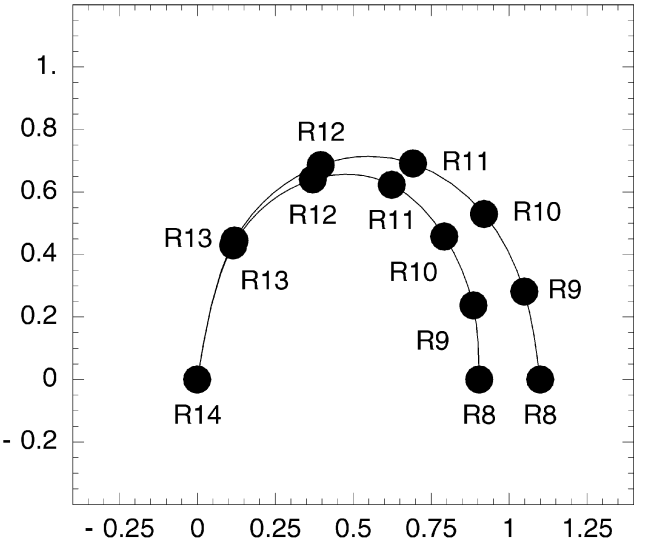

FIG. 7. As Figure 6 but for receivers 8–14.

ACKNOWLEDGMENTS

This work was financed in part by the European Union under the INCO-Copernicus project, Detection of Hydrocarbon Contaminated Soils by Electromagnetic Techniques, contract ERBIC15CT960801.

REFERENCES

Carcione, J. M., 1994, Wavefronts in dissipative anisotropic media: Geophysics, **59**, 644–657.

——— 1996, Ground penetrating radar: Wave theory and numerical simulation in lossy anisotropic media: Geophysics, **61**, 1664–1677.

Carcione, J. M., and Cavallini, F., 1993, A semi-analytical solution for the propagation of pure shear waves in dissipative monoclinic media: Acoustics Letters, **17**, 72–76.

Carcione, J. M., and Schoenberg, M., 2000, 3-D ground-penetrating radar simulation and plane-wave theory in anisotropic media: Geophysics, **65**, 1527–1541.

Carcione, J. M., Quiroga-Goode, G., and Cavallini, F., 1996, Wavefronts in dissipative anisotropic media: Comparison of the plane-wave theory with numerical modelling: Geophysics, **61**, 857–861.

Casula, G., and Carcione, J. M., 1992, Generalized mechanical model analogies of linear viscoelastic behaviour: Boll. Geof. Teor. Appl., **34**, 235–256.

Chew, W. C., 1990, Waves and field in inhomogeneous media: Van Nostrand Reinhold, New York.

Lindell, I. V., and Olyslager, F., 1997, Analytic Green dyadic for a class of nonreciprocal anisotropic media: IEEE Trans. Antennas and Propagation, **45**, 1563–1565.

Negi, J. G., and Saraf, P. D., 1989, Anisotropy in geoelectromagnetism: Elsevier Science Publ. Co., Inc.

Olhoeft, G. R., and Capron, D. E., 1994, Petrophysical causes of electromagnetic dispersion: 5th Internat. Conf. on Ground Penetrating Radar, Proceedings, 145–152.

Teixeira, F. L., and Chew, W. C., 1997, Systematic derivation of anisotropic PML absorbing media in cylindrical and spherical coordinates: IEEE Microw. Guided Wave Lett., **17**, 231–236.

——— 1998, Analytical derivation of a conformal perfectly matched absorber for electromagnetic waves: Micro. Opt. Tech. Lett., **17**, 231–236.

APPENDIX A

PLANE-WAVE ANALYSIS

Assume nonuniform harmonic plane waves with a phase factor

$$\exp(\mathrm{i}\omega\boldsymbol{\xi}\cdot\mathbf{x}), \tag{A-1}$$

where $\boldsymbol{\xi}$, the complex slowness vector, is equal to $\mathbf{k}/\omega$, with $\mathbf{k}$ and ω the wavenumber vector and frequency, respectively. The dot denotes the scalar product.

For such harmonic waves,

$$\nabla\times \;\rightarrow\; \mathrm{i}\omega\boldsymbol{\xi}\times. \tag{A-2}$$

Substituting equation (A-2) into equation (3), in the absence of sources, yields

$$\boldsymbol{\xi}\times[\boldsymbol{\epsilon}^{-1}\cdot(\boldsymbol{\xi}\times\mathbf{H})]+\boldsymbol{\mu}\cdot\mathbf{H}=0. \tag{A-3}$$

Alternatively, by duality,

$$\boldsymbol{\xi}\times[\boldsymbol{\mu}^{-1}\cdot(\boldsymbol{\xi}\times\mathbf{E})]+\boldsymbol{\epsilon}\cdot\mathbf{E}=0, \tag{A-4}$$

corresponding to three scalar equations on the components of $\mathbf{E}$:

$$\left[e_{ijk}\xi_j(\boldsymbol{\mu}^{-1})_{kl}e_{lpq}\xi_p+\epsilon_{iq}\right]E_q=0, \tag{A-5}$$

where the subindices take the values 1, 2, and 3 and e_{ijk} are the elements of the Levi-Civita tensor. These equations are analogous to the 3-D viscoelastic Christoffel equations.

So far, the dispersion relations correspond to a general (i.e., triclinic) medium. Let us consider now the orthotropic case, in which $\boldsymbol{\epsilon}$ and $\boldsymbol{\mu}$ are diagonal. Then, equation (A-5) may be written as

$$\boldsymbol{\Gamma}\cdot\mathbf{E}=\mathbf{0}, \tag{A-6}$$

where the EM Christoffel matrix is (Carcione and Schoenberg, 2000)

$$\boldsymbol{\Gamma}=\begin{pmatrix}\epsilon_1-\left(\xi_2^2/\mu_3+\xi_3^2/\mu_2\right) & \xi_1\xi_2/\mu_3 & \xi_1\xi_3/\mu_2\\ \xi_1\xi_2/\mu_3 & \epsilon_2-\left(\xi_1^2/\mu_3+\xi_3^2/\mu_1\right) & \xi_2\xi_3/\mu_1\\ \xi_1\xi_3/\mu_2 & \xi_2\xi_3/\mu_1 & \epsilon_3-\left(\xi_1^2/\mu_2+\xi_2^2/\mu_1\right)\end{pmatrix}. \tag{A-7}$$

After defining

$$\eta_i=\epsilon_i\mu_i,\qquad \zeta_i=\epsilon_j\mu_k+\epsilon_k\mu_j;\qquad i\neq j\neq k\neq i, \tag{A-8}$$

the 3-D dispersion relation, i.e., the vanishing of the determinant of the Christoffel matrix, becomes

$$\begin{aligned}&\left(\epsilon_1\xi_1^2+\epsilon_2\xi_2^2+\epsilon_3\xi_3^2\right)\left(\mu_1\xi_1^2+\mu_2\xi_2^2+\mu_3\xi_3^2\right)\\&\quad-\left(\eta_1\zeta_1\xi_1^2+\eta_2\zeta_2\xi_2^2+\eta_3\zeta_3\xi_3^2\right)+\eta_1\eta_2\eta_3=0.\end{aligned} \tag{A-9}$$

As stated in the Introduction, we see from equation (A-9) that there are only quartic and quadratic terms of the slowness components in the dispersion relation of an orthotropic medium.

The slowness vector $\boldsymbol{\xi}$ can be split in real and imaginary vectors such that $\omega\mathrm{Re}(\boldsymbol{\xi})\cdot\mathbf{x}$ is the phase and $-\omega\mathrm{Im}(\boldsymbol{\xi})\cdot\mathbf{x}$ is the attenuation. Assume that propagation and attenuation directions coincide. This is a uniform plane wave, the equivalent of a homogeneous plane wave in viscoelasticity. The slowness vector can be expressed as

$$\boldsymbol{\xi}=\xi(l_1,l_2,l_3)^\top\equiv\xi\hat{\boldsymbol{\xi}}, \tag{A-10}$$

where ξ is the complex wavenumber and $\hat{\boldsymbol{\xi}}=(l_1,l_2,l_3)^\top$ is a real unit vector, with l_i the direction cosines.

Replacing equation (A-10) into the dispersion relation (A-9) yields

$$A\xi^4-B\xi^2+\eta_1\eta_2\eta_3=0, \tag{A-11}$$

where

$$A=\left(\epsilon_1l_1^2+\epsilon_2l_2^2+\epsilon_3l_3^2\right)\left(\mu_1l_1^2+\mu_2l_2^2+\mu_3l_3^2\right) \tag{A-12}$$

and

$$B=\eta_1\zeta_1l_1^2+\eta_2\zeta_2l_2^2+\eta_3\zeta_3l_3^2. \tag{A-13}$$

We define the real wavenumber vector and the real attenuation vector as

$$\mathrm{Re}(\boldsymbol{\xi})\quad\text{and}\quad\boldsymbol{\alpha}=\omega\mathrm{Im}(\boldsymbol{\xi}), \tag{A-14}$$

respectively.

In terms of the complex velocity $V\equiv\xi^{-1}$, the phase velocity and attenuation are

$$V_p=[\mathrm{Re}(V^{-1})]^{-1}\quad\text{and}\quad\alpha=\omega\mathrm{Im}(V^{-1}), \tag{A-15}$$

respectively.

Assume, for instance, propagation in the $(1,2)$-plane. Then, $l_3=0$ and the dispersion relation (A-11) is factorable, giving

$$\left[\xi^2\left(\epsilon_1l_1^2+\epsilon_2l_2^2\right)-\epsilon_1\epsilon_2\mu_3\right]\left[\xi^2\left(\mu_1l_1^2+\mu_2l_2^2\right)-\epsilon_3\mu_1\mu_2\right]=0. \tag{A-16}$$

These factors give the TM and TE modes with complex velocities:

$$V^{\mathrm{TM}}=\left(\frac{l_1^2}{\epsilon_2\mu_3}+\frac{l_2^2}{\epsilon_1\mu_3}\right)^{1/2} \tag{A-17}$$

and

$$V^{\mathrm{TE}} = \left(\frac{l_1^2}{\mu_2 \epsilon_3} + \frac{l_2^2}{\mu_1 \epsilon_3} \right)^{1/2}. \qquad \text{(A-18)}$$

In the TM (TE) case the magnetic (electric) field vector is perpendicular to the propagation plane. For obtaining the slowness and complex velocities for the other coordinate planes, make the following subscript substitution:

$$\begin{aligned} &\text{from (1,2)-plane to (1,3)-plane:} \quad (1,2,3) \rightarrow (3,1,2), \\ &\text{from (1,2)-plane to (2,3)-plane:} \quad (1,2,3) \rightarrow (2,3,1). \end{aligned} \qquad \text{(A-19)}$$

The complex velocities (A-17) and (A-18) coincide for an orthotropic medium satisfying relations (13).